

Muonic Coulomb capture ratios and x-ray cascades in oxides

T. von Egidy, W. Denk,* R. Bergmann, H. Daniel, F. J. Hartmann, J. J. Reidy,[†] and W. Wilhelm

Physik-Department, Technische Universität München, Munich, Germany

(Received 11 August 1980)

Muonic x-ray spectra from 57 oxides have been measured with Ge detectors at the muon channel of SIN. Coulomb capture ratios and muonic x-ray intensities were deduced. A novel method was applied for oxides of heavier elements. The results exhibit for the first time systematic relations between capture ratios, the x-ray intensities in the oxidized element and in the oxygen, and the radius of the atoms. Periodic behavior with Z was established in many cases.

I. INTRODUCTION

The interaction of negative muons with solid, liquid, or gaseous matter is an interesting topic on its own. The understanding of such processes may yield information on questions in solid-state physics, atomic physics, chemistry, or biology such as atomic potentials, electron densities, atomic radii, chemical binding, or composition of compounds. Moreover, this information is often required for the interpretation of other experiments with negative muons, pions, kaons, or antiprotons which are aiming at nuclear radii, nuclear interactions, or quantum electrodynamical questions.

The Coulomb capture of negative muons proceeds via pure electromagnetic interaction. The negative muon coming from an accelerator is slowed down to an energy of less than one keV and then captured into an atomic (or molecular) orbit. It arrives at quantum states characterized by the quantum numbers (n, l) and cascades down to the $1s$ state by emission of Auger electrons or quantum radiations. Other deexcitations (nuclear excitation, neutron emission) are very rare. In a chemical compound the cascade takes place in one of the component atoms. Finally, the muon in the $1s$ state decays or interacts with the nucleus. A general discussion of the new results in the research on muons in matter can be found in the proceedings of a recent symposium.¹

Until now most of the experimental results on the Coulomb capture of negative muons were obtained by the measurement of relative intensities of muonic x rays. These intensity measurements yield two kinds of information. First, the angular momentum distribution $P(l)$ of the captured muons at a high-lying principal quantum number n can be deduced applying cascade calculations.²⁻¹⁹ Crude information as to whether the capture is preferred into low or high angular momentum states can be obtained from the $K\beta$ -to- $K\alpha$ ratio.^{13, 20-25} The distribution $P(l)$ or the ratio $K\beta$ -to- $K\alpha$ can be determined for pure elements or component atoms in a chemical compound. Second, the Coulomb capture

ratio into different atoms of a chemical compound can be obtained by the ratio of the total K -series intensities as first done by Zinov *et al.*²⁶ These experiments showed that the cascade intensities depend on the chemical structure^{4, 9, 11, 13-16, 21, 23-25, 27, 28} and that capture ratios vary more or less periodically with the atomic number Z .^{11, 26, 29-33} Although these effects are well established, only few systematic studies exist over a wide range in the periodic table.^{11, 20, 26, 31-33}

The theory of the Coulomb capture of muons was pioneered by Fermi and Teller³⁴ who suggested that the capture rate is proportional to Z ("Z law"). However, "more reliance has been placed on the result of this calculation than the authors had intended" (Ref. 27). Since the Z law failed to reproduce the experimental results,²⁹ several authors³⁶⁻³⁹ extended the calculations of Fermi and Teller. However, only recently theoretical predictions of capture ratios were published^{35, 40, 41} which include a periodic variation with Z and which give reasonable agreement with capture ratios in oxides. The "initial" angular momentum distribution $P(l)$ was previously assumed⁴²⁻⁴⁴ to have a statistical shape $P(l) \propto 2l + 1$. In order to reproduce the experimental data, a modified statistical shape $P(l) \propto (2l + 1)e^{\alpha l}$ was introduced² where α is treated as a free parameter. Systematic theoretical predictions of $K\beta$ -to- $K\alpha$ ratios or of "initial" angular momentum distributions $P(l)$ do not exist. Only a few authors^{37, 38, 45-47} performed theoretical calculations to obtain the "initial" angular momentum distribution. Their results are in most cases close to a statistical distribution.

The periodic behavior of the capture ratios was compared with the electron affinity,⁴⁸ the atomic radius,⁴¹ the atomic volume, the ionicity, the positron lifetime, and with corresponding values of pionic and kaonic x rays,^{30, 35, 49, 50} and correlations have been identified.³³ The periodic variations of the Coulomb capture ratio and of cascade intensities can be very well studied systematically for oxides, because a large number of oxides is

available and the chemical structure is sufficiently well known. Capture ratios of oxides were already reported by Sens *et al.*⁵¹ and Baijal *et al.*²⁹ who measured the different lifetimes of the muons in the 1s state. Zinov *et al.*²⁶ were the first who measured oxides systematically (with the method of the *K*-series intensities) and in this way they found the periodicity of the capture ratios. However, they used NaI detectors for the detection of the x ray. Some selected oxides were measured later with Ge(Li) detectors,^{13,24,52,53} and some discrepancies were found. Therefore, it seemed very desirable to measure as many oxides as possible with high-resolution Ge(Li) detectors in order to obtain capture ratios as well as the detailed intensity patterns of the *K* series in the oxidized element and in the oxygen. Moreover, in the present investigation a novel technique (Cu-box method) was applied for the Coulomb capture ratios of the oxides with $Z \geq 46$ which are difficult to measure with Zinov's method, because the measuring time becomes very long and the uncertainties in the efficiency calibration of the detectors and in the absorption corrections become large. A detailed description of the experiments can be found in Ref. 54. The capture ratios obtained with the Cu-box method have been slightly modified in the present paper compared with the previous publication³¹ due to an improved calibration. The empirical intensity correlations in muonic x-ray spectra of oxides deduced from the values of the present investigation have been reported.³³

II. EXPERIMENTS

All experiments were performed at the muon channel I of SIN (Swiss Institute for Nuclear Research, Villigen, Switzerland). A general description of the experimental arrangement, of the data-collection system and of the data evaluation will be published elsewhere.¹⁷ The muons, identified with a scintillation counter telescope, were slowed down by some centimeters of polyethylene and stopped in the target which was tilted to the beam axis. The spectra were measured with two types of Ge detectors, a 5-cm³ intrinsic Ge detector for $30 \text{ keV} < E_\gamma < 1 \text{ MeV}$ (850-eV FWHM at 130 keV, in beam) and a 50-cm³ Ge(Li) for $100 \text{ keV} < E_\gamma < 10 \text{ MeV}$ (2.4-keV FWHM at 1.3 MeV, in beam). As an example of the measuring conditions we give some typical rates for a proton beam of 20 μA and a muon momentum of 85 MeV/*c*: telescope $4 \times 10^4 \text{ sec}^{-1}$, small detector singles 800 sec^{-1} , and large detector singles 4000 sec^{-1} . The measuring time varied from 20 min to 36 h per target (about 30 min with the Cu-box method). The spectra in prompt coincidence with the telescope were collected with 8192-channel ADC's and stored in an

on-line computer. Delayed spectra and ungated spectra were also recorded in order to identify nuclear gamma rays and to survey the coincidence electronics, respectively. The efficiency of the detectors was determined very carefully with calibrated sources of ⁵⁷Co, ¹³³Ba, ¹³⁷Cs, and ⁶⁰Co, with a source of ⁵⁶Co, and with gamma ray intensities up to 9.7 MeV from the Cr(*n*, γ) reaction⁵⁵ (measured at the FRM reactor at Garching near Munich).

The muonic *K*-series intensities of oxides of 43 elements were measured. In six cases two different oxides of the same element were investigated. For the elements with $Z \leq 52$, Zinov's method²⁶ was applied to determine the Coulomb capture ratio. That is, this capture ratio was obtained by determining the ratio of the total *K*-series intensities of the oxidized element and of the oxygen. For elements with $Z \geq 46$, the novel Cu-box method^{31, 32, 56} was applied to obtain the capture ratios.

For the first method the targets had an area of $5 \times 7 \text{ cm}^2$. The target material had a mass of 28 g corresponding to an areal density of 0.8 g/cm^2 . The resulting target thickness was several mm. The target frame consisted of aluminum (0.5 mm thickness) covered with Mylar foil (2 μm thickness) or Al foil (10 μm thickness). Some target containers were made completely of polyethylene (for instance for the Al oxide measurement). A special Al container was constructed for technetium oxide, because only a sample of 1.6 g TcO₂ was available and because a tight container was required for this radioactive material. It consisted of a disk with 3 cm outer diameter and 1.5 cm thickness, double walls and an inner volume of 0.9 cm^3 .

The targets for the Cu-box method are described elsewhere.^{31, 56} The Cu boxes had the size $7 \times 5 \times 0.6 \text{ cm}^3$ with a wall thickness of 0.2 mm. The boxes were divided in two parts by a $7 \times 5 \times 0.04\text{-cm}^3$ Cu sheet. Both sections of the box were filled with 10 g oxide each.

In order to determine the spectrum of the background, in particular the intensity of oxygen lines in the background, special targets of boron powder, graphite, magnesium sheet and nickel sheet, respectively, were measured. Examples of measured spectra are shown in Fig. 1. For the Cu-box method, spectra were recorded only with the 5-cm³ intrinsic Ge detector, because only the region of the oxygen *K* series and of the Cu *4f-3d* transition (100–200 keV) was needed.

III. EVALUATION AND RESULTS

The spectra were analyzed for line intensities with the aid of a computer program. Gaussian

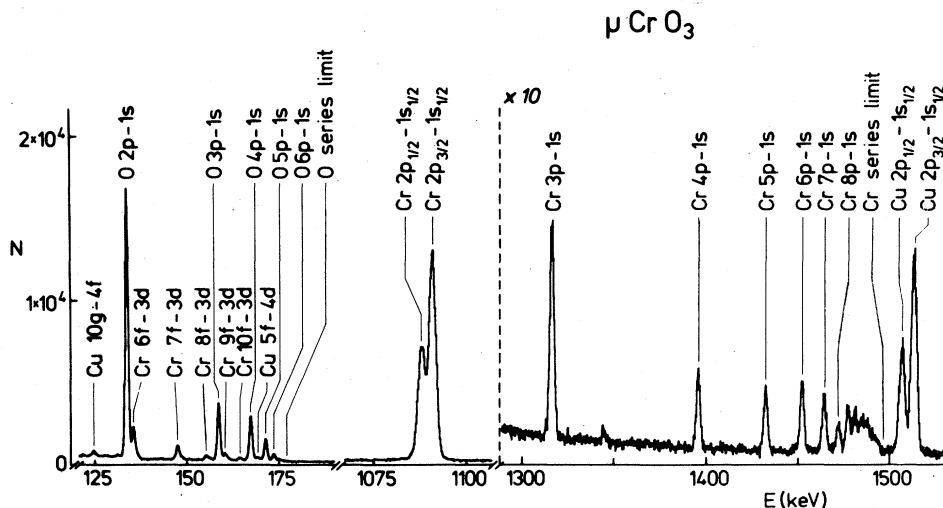


FIG. 1. Muonic x-ray spectrum of CrO_3 . The low-energy part was measured with the small detector (0.11 keV/channel), the high-energy part with the large detector (0.21 keV/channel). N = counts per channel.

line shapes with an exponential tail and with a step function under the lines were used. The intensities were corrected for detector efficiency and target self-absorption. In the cases where both the small and the large detector were used the two spectra were normalized using the strong lines appearing in both spectra, usually the $3d-2p$ transition in the oxidized element. The contribution of the background to the intensity of the oxygen K series was very carefully determined. This was achieved by comparison of telescope rates and intensities of background lines from C, N, Al, and Cu with corresponding rates and intensities of targets without oxygen (see Sec. II).

A. Capture ratios and cascade intensities obtained with Zinov's method

The Coulomb capture ratios for oxides with $Z \leq 52$ were determined by Zinov's method. The per-atom capture ratio is given for a compound $Z_k Z'_m$ by

$$A(Z, Z') = [I_{K\text{-total}}(Z) / I_{K\text{-total}}(Z')] m/k, \quad (1)$$

where $I_{K\text{-total}}(Z)$ is the total K -series intensity (not normalized) of the element Z and m/k is the stoichiometric ratio, and Z' equals 8 for oxides. The basic assumption of this formula is that all muons end up by radiative transitions in the $1s$ state. This assumption is justified in all elements we investigated with this method. The capture ratios determined with formula (1) are listed in Table I, Column 3, and marked with "Z". In three cases (CaO, SrO, BaO) the oxides are very hygroscopic and the water content was not checked; therefore only lower limits for the capture ratios are given.

Muonic x-ray intensities for the K series in the oxidized element and in the oxygen are given in Table II. In some cases the L -series intensities were also obtained (Table III). These intensities were normalized with the total K -series intensities giving intensities Y_i per captured muon in one element,

$$Y_i = I_i / I_{K\text{-total}}, \quad (2)$$

where Y_i and I_i are the normalized and measured intensities, respectively. The errors ΔY_i were calculated from the errors ΔI_i with the error propagation law yielding relatively small errors for the $2p-1s$ transitions. The errors include the contributions from the statistical error, the detector efficiency calibration (about 5%), the target self-absorption and the normalizations.

The measurement of the L series provided an internal check of the different corrections to the intensities, in particular of the detector efficiency, because the total L -series intensity has to be equal to the $2p-1s$ transition if the Auger contribution is neglected. Our results are consistent with these requirements within the error bars, in all cases.

B. Capture ratios obtained with the Cu-box method

The Coulomb capture ratio for 25 oxides was measured with the Cu-box method which is described in detail elsewhere.^{31,56} The target material is contained in a copper box. Using the intensities of the low-energy muonic x rays from copper (4-3 transition at 115 keV and 3-2 transition at 330 keV), the number of stopped muons in both components of the oxide can be derived after suitable corrections and an appropriate calibra-

TABLE I. Muonic Coulomb capture ratios in oxides.

Z	Oxide	Experimental ratios			Calculated ratios		
		Present investigation	Method ^a	Zinov <i>et al.</i> ^b	Other authors	Schneuwly <i>et al.</i> ^c	Daniel ^d
11	Na ₂ O ₂	0.99±0.05	Z		0.92±0.02 ^e		0.93
12	{MgO	0.89±0.05	Z	0.83±0.04		1.03	1.20
	{MgO ₂			0.82±0.05		1.06	(1.20)
13	Al ₂ O ₃	0.74±0.04	Z	0.85±0.06	0.65±0.06 ^f	0.87	1.43
14	{SiO ^g	0.96±0.05	Z				(1.65)
	{SiO ₂	0.84±0.04	Z	0.79±0.07	0.87±0.07 ^h	0.82	1.65
15	P ₂ O ₅ ⁱ	1.00±0.05	Z		0.93±0.10 ^f	0.93	(1.79)
20	CaO ⁱ	>1.5	Z	1.36±0.10	1.45±0.09 ^j	1.59	1.46
21	Sc ₂ O ₃			2.78±0.20		1.77	1.82
22	{TiO	2.64±0.19	Z				(2.11)
	{TiO ₂	2.70±0.13	C, Z	2.70±0.20	1.90±0.10 ^j	1.95	2.11
23	{V ₂ O ₃				2.19±0.18 ^j	2.09	(2.37)
	{V ₂ O ₄	2.70±0.19	Z		2.28±0.23 ^j	2.10	(2.37)
	{V ₂ O ₅	2.86±0.20	Z	3.10±0.20	2.68±0.14 ^j	2.12	2.37
24	{Cr ₂ O ₃	3.45±0.25	Z	3.00±0.17	2.04±0.11 ^j	2.27	2.41
	{CrO ₃ ⁱ	3.52±0.18	Z				2.56
25	MnO ₂	2.60±0.19	Z				2.59
26	Fe ₂ O ₃	3.21±0.20	C, Z			2.49	(2.73)
27	{Co ₃ O ₄	3.35±0.25	Z				(2.85)
	{Co ₂ O ₃	3.70±0.38	C			2.59	(2.85)
28	NiO _{1.57} ^k	2.66±0.20	Z				(2.94)
29	{Cu ₂ O			3.8±0.9		2.84	2.93
	{CuO	3.26±0.23	Z	3.6±0.4	6.1±0.9 ^l	2.88	(2.93)
30	ZnO	3.06±0.24	Z	2.66±0.32		2.81	2.75
31	Ga ₂ O ₃	2.77±0.20	Z				2.78
32	GeO ₂	2.90±0.21	Z				2.93
33	As ₂ O ₃	3.39±0.25	Z				(2.95)
34	SeO ₂	2.72±0.20	Z		2.91±0.11 ^e		(2.98)
38	SrO ⁱ	>1.2	Z				2.09
39	Y ₂ O ₃	2.19±0.16	Z	1.83±0.12	2.07±0.13 ^j	2.11	2.54
40	ZrO ₂	2.62±0.19	Z	2.38±0.16		2.19	2.90
41	Nb ₂ O ₅	2.95±0.23	Z				3.22
42	MoO ₃	3.60±0.29	Z	3.48±0.23		2.61	3.43
43	TcO ₂	3.26±0.31	Z				(3.59)
46	PdO	3.57±0.44	C				(3.70)
47	Ag ₂ O	3.83±0.32	Z				3.57
48	CdO	3.14±0.25	C, Z	6.7±1.5	2.47±0.22 ^j	3.10	3.34
49	In ₂ O ₃	2.92±0.31	Z	2.94±0.28		3.16	3.19
50	SnO ₂	3.02±0.23	Z	3.17±0.24		3.24	3.47
51	{Sb ₂ O ₃	3.52±0.28	Z	3.48±0.35	2.79±0.15 ^j	3.24	(3.42)
	{Sb ₂ O ₅ ⁱ			1.73±0.09		3.33	3.42
52	TeO ₂	3.22±0.25	Z				(3.44)
56	{BaO ^l	>1.6	C	2.27±0.22		2.64	2.57
	{BaO ₂	2.84±0.36	C	3.28±0.30		2.61	(2.57)
57	La ₂ O ₃	2.73±0.33	C			2.64	3.10
58	CeO ₂	4.50±0.55	C			2.86	3.44
60	Nd ₂ O ₃	5.13±0.35	C				3.30
62	Sm ₂ O ₃	4.40±0.74	C	3.09±0.34		3.25	3.41
63	Eu ₂ O ₃	4.34±0.46	C			3.36	3.45
64	Gd ₂ O ₃	5.52±0.33	C				3.47
66	Dy ₂ O ₃	5.79±0.61	C			3.74	3.60
70	Yb ₂ O ₃	6.85±0.42	C	3.18±0.34		4.28	3.80
71	Lu ₂ O ₃	5.31±0.58	C			4.42	3.84
73	Ta ₂ O ₅	7.20±0.73	C			4.78	4.62
74	WO ₃	5.75±0.67	C			4.97	4.85
81	Tl ₂ O ₃	4.81±0.57	C			4.02	4.20
82	{PbO	4.88±0.55	C	5.8±0.7		3.74	(4.15)
	{PbO ₂	5.03±0.58	C	4.17±0.30	4.56±0.53 ^l	3.83	4.15

TABLE I. (Continued).

Z	Oxide	Experimental ratios			Calculated ratios		
		Present investigation	Method ^a	Zinov <i>et al.</i> ^b	Other authors	Schneuwly <i>et al.</i> ^c	Daniel ^d
83	Bi ₂ O ₃	3.77 ± 0.43	C	4.3 ± 0.5		3.65	(4.31)
90	ThO ₂	3.57 ± 0.50	C			3.11	4.27
92	UO ₂	4.65 ± 0.55	C			3.48	(4.98)
	U ₃ O ₈	4.99 ± 0.65	C				(4.98)
	UO ₃			6.0 ± 0.5		3.56	4.98

^a C: measured with the Cu-box method; Z: measured with Zinov's *K*-series method.

^b From Zinov *et al.* (Refs. 26 and 52).

^c From Schneuwly *et al.* (Ref. 40) (version *b* of Table I).

^d From Daniel (Ref. 41), the values are in brackets if the radius does not correspond to the correct valence.

^e From Schneuwly *et al.* (Ref. 57).

^f From Sens *et al.* (Ref. 51).

^g Might contain Si + SiO₂.

^h From Mausner *et al.* (Ref. 13).

ⁱ Hygroscopic, might contain H₂O.

^j From Knight *et al.* (Ref. 24).

^k Black nickel oxide.

^l From Bajjal *et al.* (Ref. 29).

tion. The number of captures in the oxygen is obtained by summing up the oxygen *K*-series intensities. The difference between the total number of muons captured in the oxide and the number captured in oxygen is the number of muons captured in the oxidized element. The resulting capture ratios are listed in Table I, Column 3, and marked with "C." The x-ray intensities of the oxygen *K* series are given in Table II.

IV. DISCUSSION

A. Coulomb capture ratios in oxides

The Coulomb capture ratios $A(Z, Z')$ in oxides are listed in Table I together with previous results by Sens *et al.*,⁵¹ Bajjal *et al.*,²⁹ Zinov *et al.*,^{26,52} Knight *et al.*,²⁴ and Mausner *et al.*¹³ An experimental value of Schneuwly *et al.*⁵⁷ is also given for Na although this ratio is obtained as average from NaNO₂, NaNO₃, Na₂SO₃, Na₂SO₄, Na₂SeO₃, and Na₂SeO₄. The agreement is in most cases very good. The ratios of Knight *et al.* are in all cases smaller than our values.

After the completion of the present investigation a preprint of Suzuki *et al.*⁵⁸ came to our attention. These authors derived capture ratios of 22 oxides by measuring the different lifetimes. In all 15 cases which can be compared with our capture ratios the differences are larger than the summed errors, Suzuki's ratios being larger for the oxides of Al, Si, Mn, and Cu, and smaller for all other oxides. A reason for these discrepancies is not obvious. A detailed comparison is difficult be-

cause of the completely different experimental methods.

In Columns 6 and 7 of Table I, theoretical predictions by Schneuwly *et al.*⁴⁰ and Daniel⁴¹ are given. Our new experimental results and various predictions are shown in Fig. 2. It is evident that the predictions of Fermi and Teller,³⁴ Daniel,³⁶ and Vogel *et al.*^{37,38} which do not take into consideration a *Z* periodicity, fail to reproduce the experimental values although Daniel's³⁶ curve lies about in the middle of the experimental points.

Recently Daniel⁴¹ proposed a new formula for the capture ratio where the capture probability is proportional to $1/R(Z)$. $R(Z)$ is the metallic radius of the atoms for the coordination number 12 and the actual valences as summarized by Pearson⁵⁹:

$$A(Z, Z') = \frac{Z^{1/3} \ln(0.57Z)R(Z')}{Z'^{1/3} \ln(0.57Z')R(Z)}$$

Using this formula one obtains values which are in excellent agreement with the experimental values for $30 \leq Z \leq 57$ and which reproduce the general trend quite well for $20 < Z < 30$ and $Z > 57$. In the third period the agreement is very good for Na but fails by a factor of 2 for Si.

A different approach to reproduce experimental Coulomb capture ratios was recently published by Schneuwly *et al.*⁴⁰ In this method one assumes that the not too strongly bound electrons play a decisive role. In Table I and Fig. 2 we give the values of version *b* of Schneuwly *et al.* Their values are surprisingly similar to Daniel's results although the method of the calculation is completely dif-

TABLE II. Muonic *K*-series intensities in oxides normalized to the sum of the corresponding *K* series.

<i>Z</i>	Oxide	Oxidized element				Oxygen		
		<i>I</i> (2-1)	<i>I</i> (3-1)	<i>I</i> (4-1)	<i>I</i> (rest-1)	<i>I</i> (2-1)	<i>I</i> (3-1)	<i>I</i> (rest-1)
11	Na ₂ O ₂	0.772 ± 0.004	0.092 ± 0.003	0.060 ± 0.002	0.076 ± 0.003	0.631 ± 0.004	0.162 ± 0.003	0.206 ± 0.004
12	MgO	0.801 ± 0.005	0.082 ± 0.004	0.055 ± 0.003	0.062 ± 0.004	0.686 ± 0.004	0.154 ± 0.003	0.161 ± 0.003
13	Al ₂ O ₃	0.793 ± 0.005	0.080 ± 0.003	0.049 ± 0.003	0.078 ± 0.004	0.657 ± 0.004	0.167 ± 0.004	0.176 ± 0.003
14	SiO ^a	0.806 ± 0.004	0.076 ± 0.003	0.042 ± 0.002	0.077 ± 0.003	0.640 ± 0.004	0.168 ± 0.003	0.192 ± 0.004
14	SiO ₂	0.814 ± 0.006	0.075 ± 0.003	0.041 ± 0.003	0.070 ± 0.005	0.648 ± 0.004	0.165 ± 0.004	0.187 ± 0.003
15	P ₂ O ₅ ^b	0.792 ± 0.006	0.073 ± 0.004	0.040 ± 0.003	0.094 ± 0.005	0.611 ± 0.004	0.173 ± 0.003	0.216 ± 0.004
22	TiO	0.794 ± 0.004	0.070 ± 0.002	0.025 ± 0.001	0.112 ± 0.004	0.646 ± 0.006	0.160 ± 0.004	0.193 ± 0.004
22	TiO ₂	0.809 ± 0.006	0.066 ± 0.002	0.023 ± 0.001	0.102 ± 0.005	0.627 ± 0.005	0.163 ± 0.003	0.210 ± 0.005
23	V ₂ O ₄	0.768 ± 0.005	0.076 ± 0.003	0.025 ± 0.001	0.131 ± 0.005	0.600 ± 0.004	0.167 ± 0.003	0.233 ± 0.004
23	V ₂ O ₅	0.782 ± 0.007	0.074 ± 0.003	0.027 ± 0.002	0.116 ± 0.007	0.611 ± 0.004	0.164 ± 0.003	0.224 ± 0.004
24	Cr ₂ O ₃	0.776 ± 0.005	0.072 ± 0.003	0.024 ± 0.001	0.129 ± 0.004	0.570 ± 0.004	0.167 ± 0.003	0.262 ± 0.005
24	CrO ₃ ^b	0.753 ± 0.005	0.076 ± 0.003	0.029 ± 0.002	0.141 ± 0.005	0.618 ± 0.004	0.162 ± 0.003	0.221 ± 0.004
25	MnO ₂	0.741 ± 0.007	0.075 ± 0.004	0.030 ± 0.002	0.153 ± 0.006	0.522 ± 0.005	0.226 ± 0.005	0.253 ± 0.006
26	Fe ₂ O ₃	0.762 ± 0.008	0.074 ± 0.003	0.027 ± 0.001	0.136 ± 0.008	0.504 ± 0.005	0.218 ± 0.004	0.278 ± 0.005
27	Co ₃ O ₄	0.747 ± 0.006	0.076 ± 0.003	0.025 ± 0.001	0.152 ± 0.006	0.615 ± 0.006	0.176 ± 0.006	0.209 ± 0.012
28	NiO _{1.57} ^c	0.740 ± 0.006	0.077 ± 0.004	0.023 ± 0.003	0.159 ± 0.006	0.553 ± 0.005	0.203 ± 0.005	0.245 ± 0.005
29	CuO	0.770 ± 0.008	0.074 ± 0.006	0.021 ± 0.002	0.134 ± 0.007	0.557 ± 0.005	0.173 ± 0.003	0.269 ± 0.005
30	ZnO	0.807 ± 0.008	0.068 ± 0.003	0.024 ± 0.002	0.102 ± 0.008	0.641 ± 0.005	0.170 ± 0.004	0.189 ± 0.005
31	Ga ₂ O ₃	0.834 ± 0.005	0.064 ± 0.003	0.017 ± 0.002	0.085 ± 0.004	0.642 ± 0.005	0.153 ± 0.004	0.205 ± 0.005
32	GeO ₂	0.853 ± 0.004	0.066 ± 0.003	0.016 ± 0.001	0.064 ± 0.003	0.606 ± 0.005	0.165 ± 0.004	0.228 ± 0.005
33	As ₂ O ₃	0.857 ± 0.012	0.067 ± 0.003	0.014 ± 0.001	0.062 ± 0.012	0.596 ± 0.004	0.172 ± 0.004	0.232 ± 0.004
34	SeO ₂	0.836 ± 0.008	0.067 ± 0.003	0.015 ± 0.002	0.082 ± 0.009	0.573 ± 0.007	0.158 ± 0.007	0.268 ± 0.006
39	Y ₂ O ₃	0.870 ± 0.006	0.064 ± 0.004	0.012 ± 0.002	0.054 ± 0.005	0.679 ± 0.004	0.158 ± 0.003	0.163 ± 0.004
40	ZrO ₃	0.895 ± 0.006	0.055 ± 0.003	0.016 ± 0.003	0.034 ± 0.004	0.655 ± 0.004	0.164 ± 0.003	0.181 ± 0.004
41	Nb ₂ O ₅	0.867 ± 0.009	0.064 ± 0.006	0.017 ± 0.002	0.052 ± 0.007	0.624 ± 0.023	0.162 ± 0.006	0.214 ± 0.007
42	MoO ₃	0.847 ± 0.013	0.048 ± 0.010	0.026 ± 0.006	0.079 ± 0.010	0.608 ± 0.009	0.167 ± 0.006	0.224 ± 0.007
47	Ag ₂ O	0.883 ± 0.008	0.059 ± 0.005	0.012 ± 0.003	0.046 ± 0.007	0.603 ± 0.018	0.193 ± 0.008	0.205 ± 0.022
48	CdO	0.901 ± 0.010	0.049 ± 0.006	0.021 ± 0.008	0.030 ± 0.005	0.649 ± 0.061	0.148 ± 0.059	0.203 ± 0.053
49	In ₂ O ₃	0.861 ± 0.062	0.050 ± 0.007	0.017 ± 0.004	0.071 ± 0.067	0.631 ± 0.007	0.167 ± 0.005	0.202 ± 0.006
50	SnO ₂	0.921 ± 0.009	0.044 ± 0.006	0.008 ± 0.004	0.027 ± 0.006	0.591 ± 0.008	0.163 ± 0.010	0.245 ± 0.006
51	Sb ₂ O ₃	0.921 ± 0.009	0.039 ± 0.006	0.014 ± 0.003	0.025 ± 0.006	0.608 ± 0.009	0.185 ± 0.006	0.207 ± 0.010
52	TeO ₂	0.895 ± 0.010	0.060 ± 0.008	0.017 ± 0.003	0.028 ± 0.007	0.602 ± 0.006	0.194 ± 0.005	0.205 ± 0.007
56	BaO ₂					0.588 ± 0.014	0.168 ± 0.009	0.244 ± 0.010
57	La ₂ O ₃					0.617 ± 0.017	0.168 ± 0.011	0.215 ± 0.010
58	CeO ₂					0.632 ± 0.014	0.160 ± 0.009	0.208 ± 0.009
60	Nd ₂ O ₃					0.587 ± 0.013	0.171 ± 0.008	0.242 ± 0.010
63	Eu ₂ O ₃					0.618 ± 0.016	0.173 ± 0.011	0.209 ± 0.010
64	Gd ₂ O ₃					0.618 ± 0.013	0.173 ± 0.008	0.208 ± 0.010
66	Dy ₂ O ₃					0.637 ± 0.021	0.162 ± 0.015	0.201 ± 0.018
71	Lu ₂ O ₃					0.633 ± 0.022	0.172 ± 0.015	0.195 ± 0.017
73	Ta ₂ O ₅					0.610 ± 0.017	0.168 ± 0.012	0.222 ± 0.014
74	WO ₃					0.578 ± 0.015	0.176 ± 0.011	0.246 ± 0.012
81	Tl ₂ O ₃					0.492 ± 0.028	0.258 ± 0.027	0.250 ± 0.027
82	PbO					0.464 ± 0.031	0.225 ± 0.030	0.311 ± 0.030
82	PbO ₂					0.543 ± 0.020	0.184 ± 0.014	0.273 ± 0.016
83	Bi ₂ O ₃					0.510 ± 0.020	0.197 ± 0.015	0.293 ± 0.017
90	ThO ₂					0.612 ± 0.033	0.156 ± 0.013	
92	UO ₂					0.615 ± 0.020	0.163 ± 0.014	0.222 ± 0.016
92	U ₃ O ₈					0.657 ± 0.018	0.149 ± 0.012	0.194 ± 0.015

^a Might contain Si + SiO₂.^b Hygroscopic, might contain H₂O.^c Black nickel oxide.

ferent. The values obtained with Daniel's formula are in slightly better agreement with experimental values for $30 \leq Z \leq 57$. However, for $12 \leq Z \leq 15$ the values of Schneuwly *et al.* are in much better

agreement with the experimental ratios. This is due, in part, to a specially adapted value of their parameter E_c used for this region.

It can be concluded from the good agreement of

TABLE III. Muonic L -series intensities in the oxidized element.

Z	Oxide	$I(3d-2p)$	$I(4d-2p)$	$I(5d-2p)$	$I(\text{rest-}2p)$
22	TiO	0.535 ± 0.029	0.082 ± 0.004	0.041 ± 0.002	0.079 ± 0.004
22	TiO ₂	0.601 ± 0.023			
23	V ₂ O ₄	0.492 ± 0.025			
23	V ₂ O ₅	0.595 ± 0.031	0.091 ± 0.005	0.047 ± 0.003	0.056 ± 0.005
24	Cr ₂ O ₃	0.421 ± 0.021			
24	CrO ₃	0.496 ± 0.023	0.082 ± 0.004	0.040 ± 0.002	0.128 ± 0.007
25	MnO ₂	0.429 ± 0.022			
26	Fe ₂ O ₃	0.466 ± 0.034	0.074 ± 0.004	0.042 ± 0.002	0.134 ± 0.007
27	Co ₃ O ₄	0.489 ± 0.025			
28	NiO _{1.57}	0.490 ± 0.026			
29	CuO	0.484 ± 0.025			
30	ZnO	0.564 ± 0.031			
31	Ga ₂ O ₃	0.526 ± 0.027			
32	GeO ₂	0.565 ± 0.029			
33	As ₂ O ₃	0.583 ± 0.030			
34	SeO ₂	0.634 ± 0.034	0.099 ± 0.007	0.028 ± 0.002	0.064 ± 0.004
39	Y ₂ O ₃	0.809 ± 0.041			
40	ZrO ₂	0.770 ± 0.039	0.083 ± 0.005	0.036 ± 0.003	0.041 ± 0.004
41	Nb ₂ O ₅	0.772 ± 0.040			
42	MoO ₃	0.694 ± 0.036	0.080 ± 0.005	0.028 ± 0.002	0.057 ± 0.005
47	Ag ₂ O	0.755 ± 0.040	0.083 ± 0.005	0.039 ± 0.004	0.049 ± 0.006
48	CdO	0.788 ± 0.042			
49	In ₂ O ₃	0.772 ± 0.069			
50	SnO ₂	0.776 ± 0.042	0.073 ± 0.005	0.018 ± 0.005	
51	Sb ₂ O ₃	0.820 ± 0.044			
52	TeO ₂	0.830 ± 0.044	0.072 ± 0.004	0.024 ± 0.003	

both calculations with the experimental results that the basic features of the Coulomb capture of muons in oxides are now understood. One can hope that an improvement of the above-mentioned calculations will solve the remaining discrepancies.

In six cases, two oxides with different valences of the same element were measured. We do not discuss SiO in this context because the composition of SiO is not well defined⁶⁰; it may consist of Si + SiO₂. The ratios of the Coulomb capture ratios are given in Table IV. Although the effect is not significant in the individual cases, it can be stated that in all cases the oxide with the higher valence appears to have the higher capture ratio. The capture ratios of the oxides with higher valences are on the average $(3.7 \pm 1.3)\%$ larger than the capture ratios with lower valences. This is in agreement with Daniel's theory which predicts higher capture ratios for the smaller atomic radius of the oxide with the higher valence. Schneuwly *et al.* calculate capture ratios in seven cases for two oxides of the same element and obtain on the average 2% higher ratios for the higher valences. This is an additional indication that the basic assumptions of both theories are correct.

B. Intensities in muonic K and L series of oxides

The muonic x-ray intensities in the oxidized element and in the oxygen are listed in Tables II and III and plotted in Figs. 3 and 4. These figures include curves which resulted from cascade calculations with Hüfner's program.³ All these calculations start with an assumed initial principal quantum number $n = 20$ and include refilling of the electronic K shell with a rate which was set to 50% of the normal refilling rate⁶¹ of one K hole in the element ($Z-1$). The angular momentum distribution was assumed to be statistical [$P(l) = (2l+1)/400$] or constant [$P(l) = 0.05$], respectively. For the discussion of Figs. 3 and 4 one has to keep in mind that higher $K\alpha$ intensity and lower intensity of the other K -series members can be caused either by higher angular momentum l of the captured muon or by a slower refilling rate of electronic K holes created by muonic Auger transitions. Only a detailed fit of the parameters used in the cascade calculation to the experimental intensities can yield the initial angular momentum distribution $P(l)$ and the K -refilling rate. This has been done in a recent publication by our group^{12,17} for metallic Mg, Al, Fe, In, Ho, and

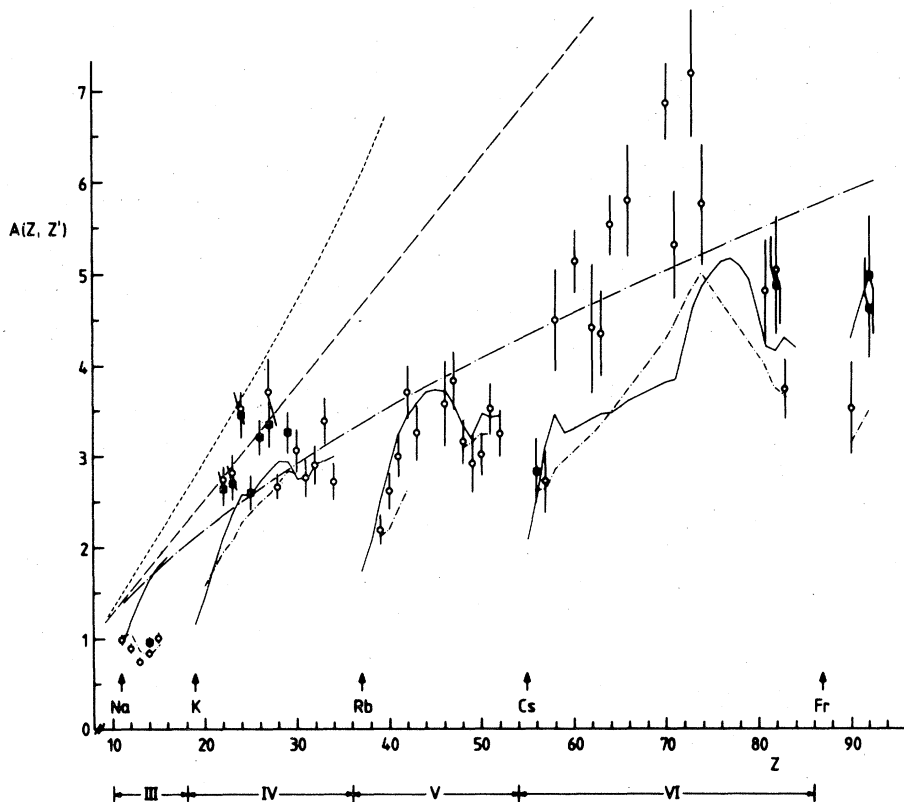


FIG. 2. Coulomb capture ratios $A(Z, Z')$, $Z'=8$, in oxides. Open circles indicate the higher-valence, full squares the lower-valence oxide. The lines correspond to the calculations by Vogel *et al.* (Ref. 37) (short dashes); Fermi and Teller's "Z law" (Ref. 34) (long dashes); Daniel (Ref. 36) (long dashes-dots); Daniel (Ref. 38) (continuous curve); and Schneuwly *et al.* (Ref. 40) (short dashes-dots). The Roman numerals indicate the respective periods of the periodic table.

Au, and it showed that the K -refilling rate is slower by a factor of about 4 for metallic Mg, Al, and Fe and corresponds about to the normal rate for metallic In, Ho, and Au. Such detailed cascade calculations have not yet been performed for oxides. The present data which include only some transitions in the K and L shells are not sufficient for this purpose.

Most theoretical calculations of $P(l)$ obtain a nearly statistical initial distribution. Only Leon and Miller⁴⁷ include a parameter which may shift the distribution to lower l values.

The inspection of Fig. 3 shows clearly that there exists a periodic variation of the muonic x-ray intensities with Z as already discussed in previous publications.^{20, 21, 25} The different intensities [$I(2-1)$, $I(3-1)$, $I(\text{rest-1})$, $I(3d-2p)$] are correlated to each other as is expected, and most of the intensities fall between the two curves calculated for statistical and constant initial distribution. The variation with Z is most pronounced for the (2-1) and (rest-1) transitions. The oxidized elements with $Z \leq 22$ have intensities which indicate that the

angular momentum distribution favors higher l values more than the statistical distribution predicts or that the electronic K -refilling rate is more strongly reduced. Indeed, the previous publication of our group¹⁷ pointed out both that for Mg and Al metals the l distribution is shifted towards higher l and that the K -refilling rate of these elements is reduced. This seems to be the case also for all oxides with $Z \leq 22$. As was discussed in Ref. 17, the reason for the reduction of the K -refilling rate of these elements is a strong depletion of the electronic L shell, because L -shell refilling is much slower than the muonic L -Auger rate. However, the refilling rates of the heavier elements are always faster than the muonic Auger rates.

The region from Cr to Cu ($24 \leq Z \leq 29$) and Mo ($Z=42$) exhibit a preference for the constant initial l distribution, that is, for lower initial l values. This is also in agreement with previous results on metallic Fe.¹² Cr and Mo are in the same group of the periodic table. Also the region from Cu to Se ($29 \leq Z \leq 34$) and the region from Ag to Te

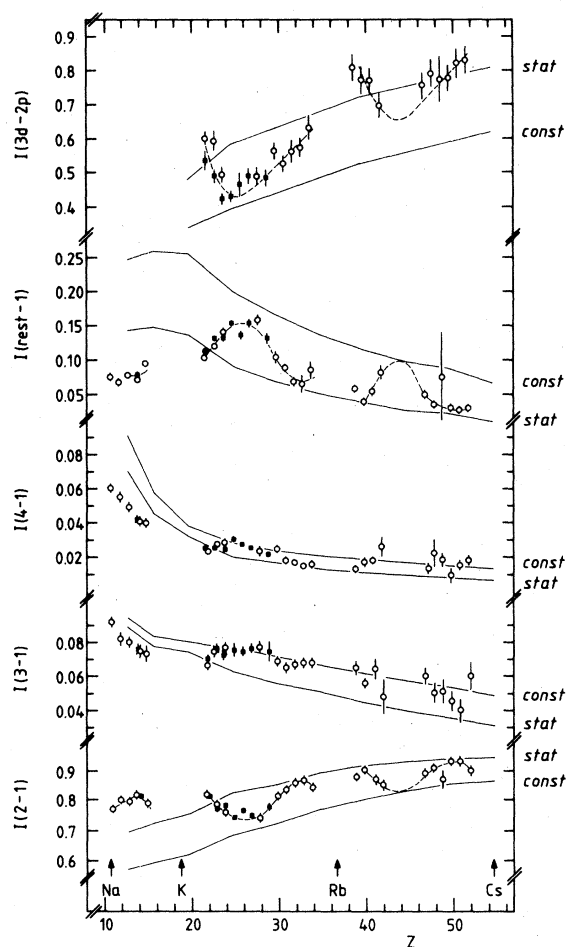


FIG. 3. Muonic K - and L -series intensities of the oxidized element. Open circles indicate the higher-valence, full squares the lower-valence oxide. These results were obtained only with Zinov's method. The full lines correspond to cascade calculations with statistical and constant initial distributions, respectively. The dashed lines are drawn to make the periodicity in the third (only Al, Si, and P can be compared), fourth, and fifth period of the periodic table more easily recognizable.

($47 \leq Z \leq 52$) which are in corresponding groups of the periodic table show exactly the same behavior. The $K\alpha$ intensity increases from Cu to As and drops to Se and it increases from Ag to Sb and drops to Te. The $K\alpha$ intensities of Al, Si, and P in the third period also show a similar behavior as the corresponding values in the fourth and fifth period (Ga, Ge, As, and In, Sn, Sb). The dashed lines in Fig. 3 indicate this periodic behavior in the third, fourth, and fifth period of the elements.

In four cases the intensities have been measured in two different oxides of the same element (Si, Ti, V, Cr). The ratios of these intensities are given in Table IV. The K -series intensities

TABLE IV. Ratios of Coulomb capture ratios of muonic x-ray intensities of oxides of the same element with different valence.

Oxides	Oxidized element				Oxygen	
	Capture ratios	(2-1)	(3-1)	(4-1)	(rest-1)	(3-1)
SiO/SiO ₂ ^a	1.14 ± 0.02	0.99 ± 0.01	1.01 ± 0.06	1.02 ± 0.09	1.10 ± 0.09	1.02 ± 0.03
TiO/TiO ₂	0.98 ± 0.02	0.98 ± 0.01	1.06 ± 0.05	1.09 ± 0.07	1.10 ± 0.07	0.98 ± 0.03
V ₂ O ₄ /V ₂ O ₅	0.94 ± 0.02	0.98 ± 0.01	1.03 ± 0.06	0.93 ± 0.08	1.13 ± 0.08	0.92 ± 0.03
Cr ₂ O ₃ /CrO ₃ ^b	0.98 ± 0.03	1.03 ± 0.01	0.95 ± 0.06	0.83 ± 0.07	0.92 ± 0.05	1.04 ± 0.03
Co ₃ O ₄ /Co ₂ O ₃	0.91 ± 0.13				0.85 ± 0.06	1.03 ± 0.03
PbO/PbO ₂	0.97 ± 0.11				0.86 ± 0.07	1.14 ± 0.13
UO ₂ /U ₃ O ₈	0.93 ± 0.10				0.94 ± 0.04	1.14 ± 0.12
average	0.963 ± 0.013	0.998 ± 0.006	1.018 ± 0.029	0.954 ± 0.040	0.995 ± 0.033	1.015 ± 0.016

^a SiO might contain Si + SiO₂. These ratios were not used for the average.

^b CrO₃ is hygroscopic. This might influence the intensities.

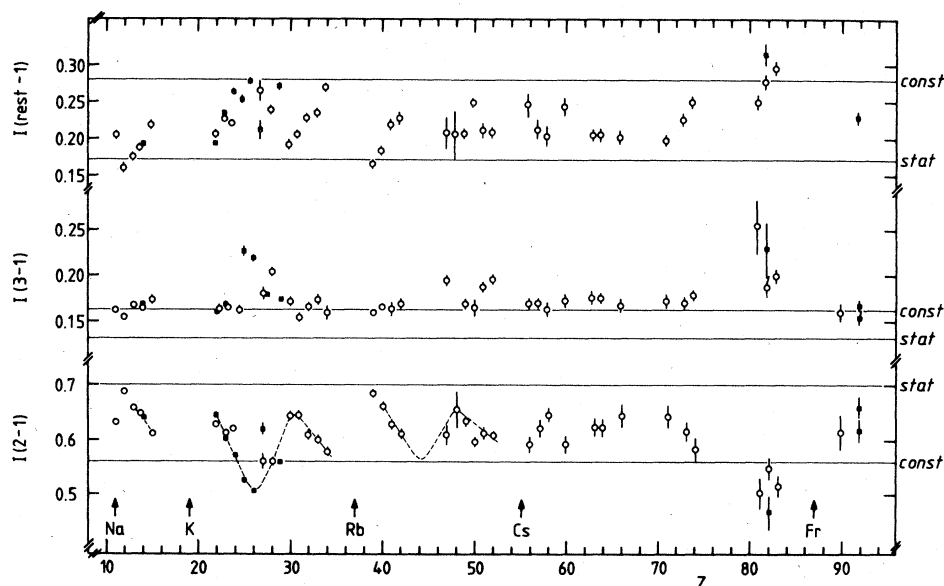


FIG. 4. Muonic K -series intensities of oxygen in oxides. These results were obtained with Zinov's method and with the Cu-box method (for further explanation see Fig. 3).

agree nearly in all cases for the different oxides, although there is a tendency that the (2-1) transitions in the oxidized element are larger for the higher oxidation and that the other K -series members are smaller for the higher oxidation. The ($3d-2p$) transitions of the higher oxidations of Ti, V, and Cr are about $(14 \pm 6)\%$ larger than the corresponding transitions of the lower oxidation. This might be an indication that at least in the oxides under consideration the higher valence favors higher angular momentum l of the captured muon and/or lower electronic refilling rate.

Figure 4 shows that the muonic K -series intensities in oxygen also fall in most cases between the lines for statistical and constant initial distribution. Only some (3-1) intensities are stronger than the predictions using a constant initial distribution, most likely because the parameters of the cascade calculations were not optimized. These intensities for oxygen also exhibit a periodic behavior with Z . This is indicated by the dashed lines. In comparing the intensities in the third, fourth, fifth, and sixth period one sees that the intensities of members of the sixth period exhibit a different behavior. It should be noted that there exists a minimum in the $K\alpha$ intensities near Fe ($Z=26$) in the oxidized element and also in the oxygen. The maxima for $K\alpha$ in the oxidized elements are near Ge ($Z=32$) and Sn ($Z=50$), while in oxygen they are found near Zn ($Z=30$) and Cd ($Z=48$).

K -series intensities of the oxygen were obtained in six cases for two different oxides of the same

element (Si, Ti, V, Cr, Pb, U). Except for the oxides of Ti one observes the same tendency as in the oxidized element that the higher oxidation is related to higher (2-1) and lower (3-1) and (rest-1) intensities (see Table IV).

The variation of the muonic cascade intensities might be related to the atomic radii^{30,49,50} as in the case of the Coulomb capture ratios,⁴¹ and comparison of Figs. 2 and 3 shows striking similarities of these values. The preferred lower l values of the captured muon in the Fe region (deduced from the lower $K\alpha$ intensity) might be caused by the smaller atomic radii of these elements. Lower angular momentum l after the μ capture can be caused by smaller impact parameter, lower momentum (energy) of the captured muon, and higher outer-electron densities. Higher outer-electron densities increase the frictional force in the outer regions of the atom where angular momentum is taken away more efficiently. Smaller atomic radii lead on the average to smaller impact parameters and higher densities of outer electrons. The similar variations with Z of the intensities in the oxidized element and in the oxygen point to a similar origin, eventually the density of the outer electrons which are, in covalent bonding, electrons common to both elements. The tendency that the higher oxidation seems to favor higher l values of the captured muon in both the oxidized element and the oxygen, is at variance with the interpretation that lower l values are caused by smaller atomic radii, because elements in higher oxidation states have smaller radii.

TABLE V. $K\beta$ -to- $K\alpha$ -ratios in oxides and pure elements (in %).

Z	Oxide	$K\beta$ -to- $K\alpha$ (oxide)		$K\beta$ -to- $K\alpha$ (metal) ^e	$\frac{K\beta\text{-to-}K\alpha\text{ (oxide)}^i}{K\beta\text{-to-}K\alpha\text{ (metal)}}$	
		This work	Other authors			
11	Na ₂ O ₂	11.92 ± 0.39		10.76 ± 0.20 ^f	1.11 ± 0.04	
12	MgO	10.24 ± 0.50		9.79 ± 0.35	1.05 ± 0.06	
13	Al ₂ O ₃	10.09 ± 0.38		9.33 ± 0.37	1.08 ± 0.06	
14	SiO	9.43 ± 0.37				
14	SiO ₂	9.21 ± 0.37	8.1 ± 0.4 ^a	9.23 ± 0.25	1.00 ± 0.05	
15	P ₂ O ₅	9.22 ± 0.51		9.26 ± 0.19	1.00 ± 0.06	
22	TiO	8.82 ± 0.25		9.88 ± 0.15	0.89 ± 0.03	
22	TiO ₂	8.16 ± 0.25	$\left\{ \begin{array}{l} 7.8 \pm 1.7^b \\ 12 \pm 1^c \\ 9.3 \pm 0.6^d \end{array} \right\}$		0.83 ± 0.03	
23	V ₂ O ₄	9.90 ± 0.39		9.6 ± 1.5 ^b	11.62 ± 0.43	0.85 ± 0.05
23	V ₂ O ₅	9.46 ± 0.38		$\left\{ \begin{array}{l} 10.0 \pm 1.1^b \\ 9 \pm 1^c \end{array} \right\}$		
24	Cr ₂ O ₃	9.28 ± 0.39	$\left\{ \begin{array}{l} 11.5 \pm 1.8^b \\ 11 \pm 1^c \end{array} \right\}$		0.71 ± 0.06	
24	CrO ₃	10.09 ± 0.40		13 ± 1 ^c	0.78 ± 0.07	
25	MnO ₂	10.12 ± 0.54		11.41 ± 0.20	0.89 ± 0.05	
26	Fe ₂ O ₃	9.71 ± 0.39		11.41 ± 0.20	0.85 ± 0.04	
27	Co ₃ O ₄	10.17 ± 0.40		13.2 ± 1.3 ^g	0.77 ± 0.08	
28	NiO _{1.57}	10.41 ± 0.55		10.39 ± 0.28	1.00 ± 0.06	
29	CuO	9.61 ± 0.78		10.14 ± 0.40	0.95 ± 0.09	
30	ZnO	8.43 ± 0.37		7.93 ± 0.30	1.06 ± 0.06	
31	Ga ₂ O ₃	7.67 ± 0.36				
32	GeO ₂	7.74 ± 0.35		7.06 ± 0.16	1.10 ± 0.06	
33	As ₂ O ₃	7.82 ± 0.35		7.21 ± 0.20	1.08 ± 0.06	
34	SeO ₂	8.01 ± 0.36		6.99 ± 0.21	1.15 ± 0.06	
39	Y ₂ O ₃	7.36 ± 0.46	5.2 ± 1.3 ^b	7.06 ± 0.24	1.04 ± 0.07	
40	ZrO ₂	6.15 ± 0.34				
41	Nb ₂ O ₅	7.38 ± 0.70		7.07 ± 0.27	1.04 ± 0.11	
42	MoO ₃	5.7 ± 1.2		7.8 ± 0.6 ^h	0.70 ± 0.15	
47	Ag ₂ O	6.68 ± 0.57				
48	CdO	5.44 ± 0.67	5.2 ± 2.6 ^b	5.86 ± 0.42	0.93 ± 0.13	
49	In ₂ O ₃	5.81 ± 0.81		4.81 ± 0.37	1.21 ± 0.21	
50	SnO ₂	4.78 ± 0.65				
51	Sb ₂ O ₃	4.23 ± 0.65				
52	TeO ₂	6.70 ± 0.90				

^a From Mausner *et al.* (Ref. 13).^b From Knight *et al.* (Ref. 24).^c From Zinov *et al.* (Ref. 21).^d From Kessler *et al.* (Ref. 4).^e From Bergmann *et al.* (Ref. 25).^f From Kaeser *et al.* (Ref. 16).^g From Quitmann *et al.* (Ref. 20).^h This value was corrected compared to Ref. 25.ⁱ Oxide data from this work, metal data from Bergmann *et al.* (Ref. 25).

C. $K\beta$ -to- $K\alpha$ ratios in oxides and pure elements

The determination of absolute intensities in the K series requires the measurement and careful evaluation of all transitions in the K series. Therefore, many authors calculate only the $K\beta$ -to- $K\alpha$ ratio [$I(3-1)/I(2-1)$] because many of the necessary corrections become small for this ratio. This ratio is also an indication whether the muon is captured preferably with high l (low $K\beta$ -to- $K\alpha$) or low l (high $K\beta$ -to- $K\alpha$). In addition

to this, fast electronic refilling increases $K\beta$ -to- $K\alpha$ and vice versa. In order to compare our intensities with previous measurements, our $K\beta$ -to- $K\alpha$ values of the oxidized elements are given in Table V together with previous $K\beta$ -to- $K\alpha$ ratios of oxides and $K\beta$ -to- $K\alpha$ ratios of pure elements²⁵ which were also measured by our group. Our results of oxides are in good agreement with most of the previous values.^{4,13,21,24} The last column in Table V gives the ratios of $K\beta$ -to- $K\alpha$ (oxide) to $K\beta$ -to- $K\alpha$ (pure element). The $K\beta$ -to- $K\alpha$ ratios

for oxides and pure elements are shown in Fig. 5. The curves from cascade calculations for statistical and constant initial distribution are also drawn. The periodic variation of $K\beta$ -to- $K\alpha$ can be seen by comparison of the values in the fourth and fifth period. A remarkable feature of the $K\beta$ -to- $K\alpha$ ratios is the fact that for $Z \leq 15$ and $Z \geq 30$, $K\beta$ -to- $K\alpha$ of oxides is larger in most cases than the one for pure elements, while for $22 \leq Z \leq 29$, $K\beta$ -to- $K\alpha$ of the pure elements is larger. It can be stated that in most cases the periodic variation of $K\beta$ -to- $K\alpha$ is less pronounced in the oxides than in the pure elements indicating a moderating influence of the oxygen.

It is a simple argument that the electronic re-filling rate might be faster in good conductors than in good insulators, leading to larger $K\beta$ -to- $K\alpha$ ratios for conductors. The comparison of the $K\beta$ -to- $K\alpha$ ratios proves that this argument is not valid in most cases and that the conductivity plays no essential role for the cascade intensities and for the initial l distribution, because the ratios of the metals are sometimes larger, sometimes smaller than the ones of the oxides. This was recently also concluded by Kaeser *et al.*¹⁶ It was already pointed out¹ that a major influence of the conductivity is very unlikely, because an effect is only expected if several electrons are missing and this is improbable in solids.

D. Correlations between the capture ratios, the muonic K -series intensities, the atomic radius, and the ionicity

The comparison of Figs. 2-5 demonstrates that there exist many correlations and anticorrelations between the capture ratios and the muonic K -series intensities. The origin of these relations is the common dependence on periodic properties of the atoms. Additional correlations of these quantities exist with the atomic radii and the ionicity. These correlations of the present data have been calculated applying mathematical correlation theory.⁶² The results are already published.³³ It could be shown that there exist general correlations between the cascade intensities of the oxidized element and of the oxygen. A main result was that after correction for the common Z dependence a strong negative correlation appeared between the capture ratios and the atomic radius R . This finding was explained⁴¹ by showing that the capture ratio is proportional to $1/R$.

V. CONCLUSION

The present publication gives for the first time a rather complete view of the Coulomb capture ratios and the muonic x-ray intensities in the oxides. The Coulomb capture ratios are in the fourth period in quantitative agreement with Daniel's calculations and in the other cases in

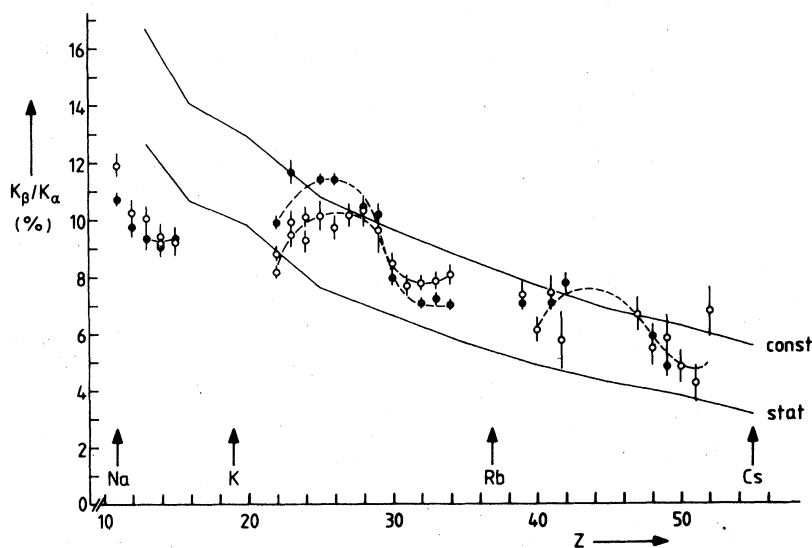


FIG. 5. $K\beta$ -to- $K\alpha$ ratios in oxides and pure elements. The open circles are the ratios of oxides, the full ones of the respective pure elements. The curves have the same meaning as in Fig. 3. The two dashed curves in the fourth period ($19 \leq Z \leq 36$) indicate the difference between the oxides and the pure elements.

qualitative agreement with the predictions of Daniel and Schneuwly *et al.* A very good test for the dependence on the atomic radius would be the measurement of the capture ratios in the alkali and alkaline-earth elements, because they have larger radii than the other neighboring elements. We give in our tables only values for Na, Mg, and Ba, because the other alkali or alkaline-earth oxides are either difficult to obtain or extremely hygroscopic. Water content modifies all intensity ratios. It is planned to measure also the capture ratios and cascade intensities in the remaining alkali and alkaline-earth elements.

Periodic behavior was also identified in the *K*- and *L*-series intensities of the oxidized element and in the *K*-series intensities of oxygen. The observed intensities vary essentially in a smooth way with *Z* and show also in detail very similar variations in the third, fourth, and fifth period (see Figs. 3 and 4). The variations are probably also related to the atomic radii.

The observed periodic variation of capture ratios

and muonic intensities in oxides give a clear indication that the Coulomb capture process of muons is to a large extent determined by the structure or density of the outer electrons of the elements. However, the small variation of the capture ratio in oxides of the same element with different valence $[(3.7 \pm 1.3)\%]$ demonstrates that the valence electrons play only a minor role. A similar statement is valid for the cascade intensities. It was also shown that the conductivity does not essentially influence the muonic cascade.

ACKNOWLEDGMENTS

We wish to thank H. Angerer, H. Hagn, and P. Stoeckel for essential technical assistance and the SIN for kind hospitality and support. The work was supported by the German Bundesministerium für Forschung und Technologie. The help of Dr. U. Wagner in the preparation of the TcO_2 target is highly acknowledged.

*Present address: Gesellschaft für Reaktorsicherheit, 8046 Garching, Germany.

†Present and permanent address: University of Mississippi, University, Miss.

¹H. Daniel, in *Proceedings of the International Symposium on Meson Chemistry and Mesomolecular Processes in Matter*, edited by V. N. Pokrovskij (Joint Institute for Nuclear Research, Dubna, USSR, 1977).

²Y. Eisenberg and D. Kessler, *Nuovo Cimento* **19**, 1195 (1961).

³J. Hüfner, *Z. Phys.* **195**, 365 (1966); and Program CASCADE.

⁴D. Kessler, H. L. Anderson, M. S. Dixit, H. J. Evans, R. J. McKee, C. K. Hargrove, R. D. Barton, E. P. Hincks, and J. D. M. Andrew, *Phys. Rev. Lett.* **18**, 1179 (1967).

⁵A. Suzuki, *Phys. Rev. Lett.* **19**, 1005 (1967).

⁶H. Koch, G. Poelz, H. Schmitt, L. Tauscher, G. Backenstoss, S. Charalambus, and H. Daniel, *Phys. Lett. B* **28**, 279 (1968).

⁷H. Backe, *Z. Phys.* **241**, 435 (1971).

⁸H. Backe, R. Engfer, H. Jahnke, E. Kankeleit, R. M. Pearce, C. Petitjean, L. Schellenberg, H. Schneuwly, W. U. Schröder, H. K. Walter, and A. Zehnder, *Nucl. Phys. A* **189**, 472 (1972).

⁹A. D. Konin, V. N. Pokrovsky, L. I. Ponomarev, H. Schneuwly, V. G. Zinov, and I. A. Yutlandov, *Phys. Lett. A* **50**, 57 (1974).

¹⁰H. J. Pfeiffer, K. Springer, and H. Daniel, *Nucl. Phys. A* **254**, 433 (1975).

¹¹A. Brandao d'Oliveira, H. Daniel, and T. von Egidy, *Phys. Rev. A* **13**, 1772 (1976).

¹²F. J. Hartmann, T. von Egidy, R. Bergmann, M. Kleber, H. J. Pfeiffer, K. Springer, and H. Daniel, *Phys. Rev. Lett.* **37**, 331 (1976).

¹³L. F. Mausner, R. A. Naumann, J. A. Monard, and S. N. Kaplan, *Phys. Rev. A* **15**, 479 (1977).

¹⁴C. R. Cox, G. W. Dogson, M. Eckhause, R. D. Hart, J. R. Kane, A. M. Rushton, R. T. Siegel, R. E. Welsh, A. L. Carter, M. S. Dixit, E. P. Hincks, C. K. Hargrove, and H. Mes, *Can. J. Phys.* **57**, 1746 (1979).

¹⁵K. Kaeser, T. Dubler, B. Robert-Tissot, L. A. Schaller, L. Schellenberg, and H. Schneuwly, *Helv. Phys. Acta* **52**, 238 (1979).

¹⁶K. Kaeser, B. Robert-Tissot, L. A. Schaller, L. Schellenberg, and H. Schneuwly, *Helv. Phys. Acta* **52**, 304 (1979).

¹⁷F. J. Hartmann, R. Bergmann, H. Daniel, H. J. Pfeiffer, T. von Egidy, and W. Wilhelm (unpublished).

¹⁸V. R. Akylas, Ph.D. thesis, California Institute of Technology, 1978 (unpublished).

¹⁹P. Vogel, *Phys. Rev. A* **22**, 1600 (1980).

²⁰D. Quitmann, R. Engfer, U. Hegel, P. Brix, G. Backenstoss, K. Goebel, and B. Stadler, *Nucl. Phys.* **51**, 609 (1964).

²¹V. G. Zinov, A. D. Konin, A. I. Mukhin, and R. V. Polyakova, *Yad. Fiz.* **5**, 591 (1967) [*Sov. J. Nucl. Phys.* **5**, 420 (1967)].

²²H. Koch, M. Krell, Ch. von der Malsburg, G. Poelz, H. Schmitt, L. Tauscher, G. Backenstoss, S. Charalambus, and H. Daniel, *Phys. Lett. B* **29**, 140 (1969).

²³L. F. Mausner, R. A. Naumann, J. A. Monard, and S. N. Kaplan, *Phys. Lett. B* **56**, 145 (1975).

²⁴J. D. Knight, C. J. Orth, M. E. Schillaci, R. A. Naumann, H. Daniel, K. Springer, and H. B. Knowles, *Phys. Rev. A* **13**, 43 (1976).

²⁵R. Bergmann, H. Daniel, T. von Egidy, F. J. Hartmann, J. J. Reidy, and W. Wilhelm, *Z. Phys. A* **291**, 129 (1979).

²⁶V. G. Zinov, A. D. Konin, and A. I. Mukhin, *Yad. Fiz.*

- 2, 859 (1965) [Sov. J. Nucl. Phys. 2, 613 (1966)].
- ²⁷H. Daniel, H. Koch, G. Poelz, H. Schmitt, L. Tauscher, G. Backenstoss, and S. Charalambus, Phys. Lett. B 26, 281 (1967).
- ²⁸T. Dubler, K. Käser, B. Robert-Tissot, L. A. Schaller, L. Schellenberg, and H. Schneuwly, Phys. Lett. A 57, 325 (1976).
- ²⁹J. S. Baijal, J. A. Diaz, S. N. Kaplan, and R. V. Pyle, Nuovo Cimento 30, 711 (1963).
- ³⁰R. Kunselmann, J. Law, M. Leon, and J. Miller, Phys. Rev. Lett. 36, 446 (1976).
- ³¹H. Daniel, W. Denk, F. J. Hartmann, J. J. Reidy, and W. Wilhelm, Phys. Lett. B 71, 60 (1977).
- ³²W. Wilhelm, R. Bergmann, G. Fottner, F. J. Hartmann, J. J. Reidy, and H. Daniel, Chem. Phys. Lett. 55, 478 (1978).
- ³³H. Daniel, W. Denk, F. J. Hartmann, W. Wilhelm, and T. von Egidy, Phys. Rev. Lett. 41, 853 (1978).
- ³⁴E. Fermi and E. Teller, Phys. Rev. 72, 399 (1947).
- ³⁵M. Y. Au-Yang and M. L. Cohen, Phys. Rev. 174, 468 (1968).
- ³⁶H. Daniel, Phys. Rev. Lett. 35, 1649 (1975).
- ³⁷P. K. Haff, P. Vogel, and A. Winther, Phys. Rev. A 10, 1430 (1974).
- ³⁸P. Vogel, P. K. Haff, V. Akylas, and A. Winther, Nucl. Phys. A 254, 475 (1975).
- ³⁹P. Vogel, A. Winther, and V. Akylas, Phys. Lett. B 70, 39 (1977).
- ⁴⁰H. Schneuwly, V. I. Pokrovsky, and V. I. Ponomarev, Nucl. Phys. A 312, 419 (1978).
- ⁴¹H. Daniel, Z. Phys. A 291, 29 (1979).
- ⁴²A. H. de Borde, Proc. Phys. Soc. London Sec. A 67, 57 (1954).
- ⁴³M. Demeur, Nucl. Phys. 1, 516 (1956).
- ⁴⁴M. B. Stearns and M. Stearns, Phys. Rev. 105, 1573 (1957).
- ⁴⁵R. A. Mann and M. E. Rose, Phys. Rev. 121, 293 (1960).
- ⁴⁶M. Leon and R. Seki, Nucl. Phys. A 282, 445 (1977).
- ⁴⁷M. Leon and J. H. Miller, Nucl. Phys. A 282, 461 (1977).
- ⁴⁸V. D. Bobrov, V. G. Varlamov, Yu. M. Grashin, B. A. Dolgoshein, V. G. Kirillov-Ugryumov, V. S. Roganov, A. V. Samoilo, and S. V. Somov, Zh. Eksp. Teor. Fiz. 48, 1197 (1965) [Sov. Phys.—JETP 21, 798 (1965)].
- ⁴⁹G. T. Condo, Phys. Rev. Lett. 33, 126 (1974).
- ⁵⁰G. L. Godfrey and C. E. Wiegand, Phys. Lett. B 56, 255 (1975).
- ⁵¹J. C. Sens, R. A. Swanson, V. L. Telegdi, and D. D. Yovanovitch, Nuovo Cimento 7, 536 (1957).
- ⁵²V. G. Zinov, A. K. Kachalkin, L. N. Nikityuk, V. N. Pokrovskij, V. N. Rybakov, and I. A. Yutlandov, in Ref. 1, p. 150.
- ⁵³L. Tauscher, G. Backenstoss, S. Charalambus, H. Daniel, H. Koch, G. Poelz, and H. Schmitt, Phys. Lett. A 27, 581 (1968).
- ⁵⁴W. Denk, Ph.D. thesis, Technische Universität München, Munich, 1979 (unpublished).
- ⁵⁵G. D. Loper and G. E. Thomas, Nucl. Instrum. Methods 105, 453 (1972).
- ⁵⁶H. Daniel *et al.* (unpublished).
- ⁵⁷H. Schneuwly, T. Dubler, K. Kaeser, B. Robert-Tissot, L. A. Schaller, and L. Schellenberg, Phys. Lett. A 66, 188 (1978).
- ⁵⁸T. Suzuki, R. J. Mikula, D. M. Garner, D. G. Fleming, and D. F. Measday, Phys. Lett. B 95, 202 (1980).
- ⁵⁹W. B. Pearson, *The Crystal Chemistry and Physics of Metals and Alloys* (Wiley, New York, 1972), p. 151.
- ⁶⁰E. G. Rochow, in *Comprehensive Inorganic Chemistry*, edited by J. C. Bailar *et al.* (Pergamon, Oxford, 1973), Vol. I, p. 1353.
- ⁶¹O. Keski-Rahkonen and M. O. Krause, At. Data Nucl. Data Tables 14, 139 (1974).
- ⁶²B. L. van der Waerden, *Mathematische Statistik*, 3rd ed. (Springer, Berlin, 1971), Chap. 13.